Optical Response of Liquid Acetonitrile at Ambient Conditions: The Dynamical Dielectric Behavior from Ab Initio Calculations

F. de Brito Mota and Roberto Rivelino*

Instituto de Física, Universidade Federal da Bahia, 40210-340 Salvador, Bahia, Brazil

Received: March 20, 2009

We probe the linear optical properties of the neat liquid acetonitrile (CH_3CN) at ambient conditions using ab initio density functional theory. Uncorrelated structures extracted from Monte Carlo simulation are employed to efficiently calculate average electronic properties. It becomes evident that condensation leads to a conduction band with a large degree of dispersion, which is consistent with the description of dipolar liquids. This allows an interpretation of the dielectric spectrum based on the electronic structure of liquid CH_3CN, and clearly shows the influence of intermolecular interactions in the absorption features. We find that the lowest-lying excitation of the condensed phase occurs at 7.8 eV, which is reasonable as compared to the 8−9.5 eV absorption region measured in the gas phase.

Introduction

Akin to water, acetonitrile (CH_3CN) forms a highly polar liquid phase at ambient conditions, which is capable of dissolving a variety of materials and promoting diverse organic synthesis.[1,2] Furthermore, neat liquid CH_3CN has been recognized as an important dielectric medium to investigate excess electron localization.[3−5] Although the solvation process relies on the dielectric behavior of the liquid, the dielectric function of acetonitrile is not yet fully understood in the electronic absorption region. To date, high resolution photoabsorption experiments have been carried out only in the gas phase with different pressure conditions.[6] Also, computational simulations of its condensed phase have focused on the molecular static electric properties.[7,8] For this reason, complementary information on the dielectric spectrum of the CH_3CN fluid phase in the optical region is timely and fundamental for advances in these research fields.[9]

From a theoretical point of view, the grand challenge is to generate the appropriate liquid structure of a complex disordered system such as acetonitrile. Therefore, the most common procedures to compute the electric susceptibilities of solutions and pure liquid CH_3CN have considered ab initio methods developed in the continuum approach.[10,11] These models, however, ignore the structural features of the medium, missing effects due to long-range intermolecular interactions. On the other hand, polar and aprotic liquids such as CH_3CN can give rise to local structures,[7,12] as pointed out by hyper-Rayleigh scattering experiments.[13] Fortunately much of the structural effects of liquid acetonitrile may be tackled via atomistic simulations.[14−16]

As state-of-the-art procedures in condensed matter theory, fully ab initio schemes based on density-functional-theory (DFT) approaches[17−20] have been employed to obtain, for example, diverse properties of liquid water, using small supercells and sampling the Brillouin zone (BZ) at the Γ-point. Nevertheless, as demonstrated by Prendergast et al.,[17] the electronic density of states of liquid water is sensitive to finite size effects. In the case of acetonitrile, these calculations would require a very large unit cell, leading to a prohibitive computational cost. A viable procedure has been to employ DFT, within the generalized gradient approximation (GGA), to compute the electronic properties of selected configurations using classical trajectories to represent the liquid. In this way, Garbuio et al.[21] have successfully calculated the optical spectrum of liquid water.

In this paper, our strategy is to perform a large scale efficient computational simulation to unveil the electronic structure and the linear optical properties of liquid acetonitrile. We employ a sequential protocol,[22,23] combining Monte Carlo (MC) simulation and first-principles DFT calculations to describe the electronic structure of the whole liquid acetonitrile at ambient conditions. Thus, within the linear response theory,[24] we obtain the frequency-dependent polarizability and the imaginary part of the dielectric function of the condensed phase from the ground-state electron density.

Computational Approach

The ground-state electronic structure of the condensed phase is calculated with the Perdew, Burke, and Ernzerhof GGA exchange-correlation functional (PBE)[25] with norm-conserving pseudopotentials.[26] The Kohn−Sham (KS) eigenstates are expanded on a basis set of atomic orbitals with double-ζ quality and polarization function, as implemented in the SIESTA code.[27] Hence, the electronic properties of the liquid state are obtained using a single *k*-point ($\mathbf{k} = \mathbf{0}$) to approximate the BZ integration. An equivalent plane-wave cutoff radius of 200 Ry for the grid integration is utilized to represent the charge density.

As input of the DFT calculations, we use statistically uncorrelated configurations generated from a standard *NPT* Metropolis MC simulation[28] carried out over 500 CH_3CN molecules at $T = 300$ K and atmospheric pressure. Using the energy autocorrelation function (further details are found in ref 23), we select configurations with less than 15% correlation. During the simulation,[29] each CH_3CN molecule is assumed to be in a rigid C_{3v} geometry having a six-site potential model[14,15] and the intermolecular interactions are described with the usual Lennard-Jones plus Coulomb potential. Both static and dynamical properties have been well reproduced in the literature using these potentials.[14,16] From the calculated center-of-mass radial

* To whom correspondence should be addressed. E-mail: rivelino@ufba.br (R.R.). Fax: +55-71-3283-6606.

10.1021/jp902549y CCC: $40.75
Published on Web 06/23/2009

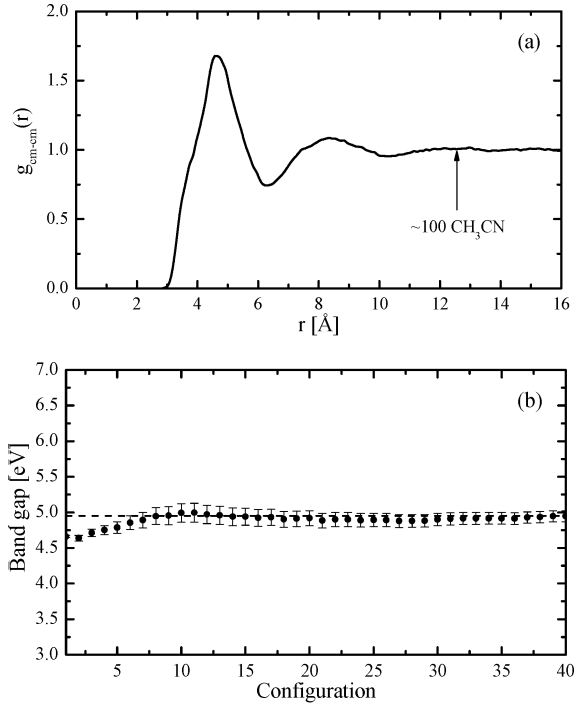

Figure 1. Calculated (a) center-of-mass radial distribution function of liquid acetonitrile from the MC simulation and (b) convergence of the configuration-averaged HOMO−LUMO band gap with DFT/PBE.

distribution function (Figure 1a), we extract samples containing 100 CH_3CN molecules, which include the bulk extrapolation, to represent the condensed phase.

The optical response of the liquid system is investigated using the approximate dielectric function, which is calculated from the matrix elements of the position operator between occupied and unoccupied eigenfunctions of the self-consistent KS Hamiltonian at the first-order time-dependent perturbation theory. Corrections due to nonlocality of the pseudopotentials are usually introduced[27] in these calculations. In this way, we obtain the imaginary part of the dielectric function, ε_2, and calculate the real part, ε_1, using Kramers−Kronig transformations.

Results and Discussion

In Figure 1b, we examine the convergence of the band gap with respect to the number of uncorrelated configurations included in the averaging. Within this scheme, the configuration-averaged HOMO−LUMO gap[30] turned out to be 4.95 ± 0.08 eV, over a Markov chain containing 40 configurations. As expected in KS-DFT calculations, and as we shall see in the following, this value of ∼5 eV should underestimate the optical gap of liquid acetonitrile. Nonetheless, correcting the KS energy levels to include many-body effects[21,31] in the electronic excitations of acetonitrile is not feasible here, because of the large number of explicit molecules in the samples (i.e., 1600 valence electrons) and different configurations of the liquid phase (ca. 40 sequential DFT calculations on average).

We emphasize that the average density of states (DOS) of the liquid phase is completely converged (see Figure 2). We also observe a large dispersion in the conduction band and no separation of the LUMO from the rest of the unoccupied KS states, as calculated for the isolated CH_3CN molecule. In the case of the isolated monomer, this separation is of ∼1.8 eV. Our observation is consistent with other DFT results obtained for liquid water considering very large supercells. As discussed

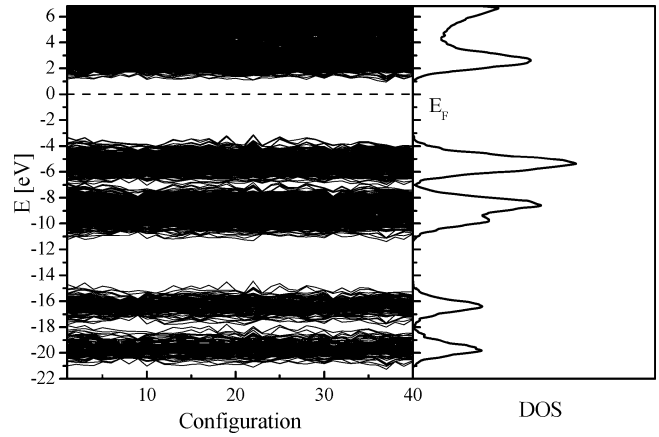

Figure 2. Convergence of the computed DFT/PBE electronic structure and DOS of liquid acetonitrile using only the Γ-point. Our zero energy scale is adjusted using the Fermi energy level E_F (dashed line).

in ref 17, small supercell calculations with $\mathbf{k} = \mathbf{0}$ lead to a separate LUMO from the conduction band of the liquid system. This artifact can be overcome, however, by increasing the *k*-point sampling, which is an accurate approximation of the DOS for larger supercells computed using a single *k*-point. In our case, considering several configurations with 100 CH_3CN molecules sampled at the Γ-point, we obtain a fine description of both the valence and conduction band of the liquid acetonitrile (Figure 2). This indicates that our average DOS is sufficiently accurate to treat the electronic unoccupied states of the liquid and, therefore, a suitable starting point to compute its absorption and dielectric response.

To understand the features of the optical absorption spectrum of the liquid, we examine first the charge density distribution related to the KS eigenstates near the Fermi level for a random configuration extracted from the MC simulation, as shown in Figure 3. We notice that the HOMO of the liquid phase (Figure 3a) is entirely delocalized over the simulation cell and dominated by π states with C≡N bonding character mixed with lone pairs (n) of the nitrogen atoms with contribution of all CH_3CN molecules. This delocalization of the HOMO is typical for each of the uncorrelated MC configurations examined here.

Interestingly, the HOMO−2 and HOMO−3 of the isolated molecule have merged together in the liquid (Figure 3b) to give a disperse band in the range −11 to −7 eV (see the DOS in Figure 2). In contrast, the LUMO of the liquid system (Figure 3c) is delocalized on the molecules, although dominated by π^* states with C−N antibonding character. Also, the LUMO+1 is delocalized on the molecules and presents σ^* states with C−C/C−H antibonding character. Although the unoccupied KS-eigenstates subspace is similar to the one calculated in the gas phase, we note that the conduction band in the liquid presents a large degree of dispersion without separation of the lowest conduction band. These findings are consistent with the description of dipolar liquids and will be valuable to interpret the transition bands in the calculated optical spectrum (Figure 3d).

The optical response is obtained from the dipolar transition matrix elements between occupied and unoccupied self-consistent KS eigenstates, considering corrections due to the nonlocality of the pseudopotentials.[27] Although this formalism is a first approximation for the excited-state properties,[32] we have to stress here that our aim has been to compute the average absorption spectrum taking into account several uncorrelated structures converging to represent the liquid. The lower energy feature of the condensed phase is mainly associated with $\pi \rightarrow$

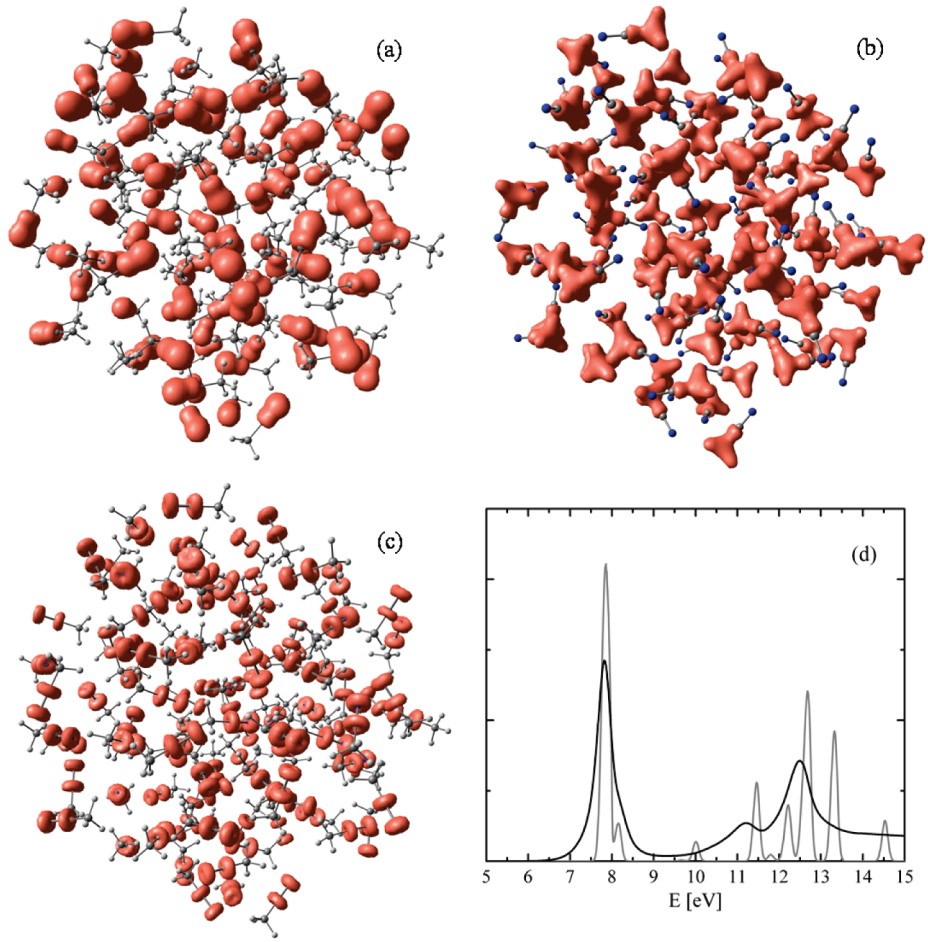

Figure 3. Isosurfaces (0.08 au) of the probability density of the Kohn−Sham eigenstates near the Fermi level calculated at the Γ-point for a single MC configuration containing 100 CH_3CN molecules: (a) the 2-fold degenerate HOMO; (b) the merged HOMO−2 + HOMO−3; (c) the 2-fold degenerate LUMO. CH_3CN molecules are indicated using gray (carbon), white (hydrogen), and blue (nitrogen) ball-and-stick models. (d) Calculated optical spectra of liquid (black line) and gaseous (gray line) acetonitrile.

π^* and $n \rightarrow \pi^*$ orbital promotions, giving a strongly absorbing peak at 7.8 eV. This spectral region contains the bulk of the valence transition bands and is consistent with the trends observed experimentally in photoabsorption spectra of gaseous CH_3CN from low to high pressures.[6] However, the intermolecular interactions in the liquid induce a significant broadening of the energy levels relative to the isolated molecule, leading to absorption peaks more red-shifted in comparison to the gas phase absorption, which is measured in the 8−9.5 eV region.[6]

Usually, the assignment of the observed bands is not a simple task and analysis is complicated by some mixing of valence and Rydberg transitions.[6] Thus, we can not assign all of these transitions from occupied to unoccupied bands at this level of calculation. Figure 3d shows the calculated optical spectra for the liquid and gas phases. The absorption intensity decreases by increasing the photo energy with no noticeable absorption peak beyond 12.5 eV. Features at higher energy in the liquid phase could correspond to $\pi \rightarrow \sigma^*$ and $n \rightarrow \sigma^*$ transitions or bands from more internal orbitals.

The positions of the two peaks at 11.2 and 12.5 eV in the liquid are not the same as calculated for the isolated molecule. This suggests either that similar transitions are occurring at different energy regions in the liquid and gas or probably that other transitions are involved in the condensed phase. This analysis becomes more complicated in the liquid, where excitonic and intraband transitions mediated by finite temperature are likely to occur.[33] Our treatment does not permit

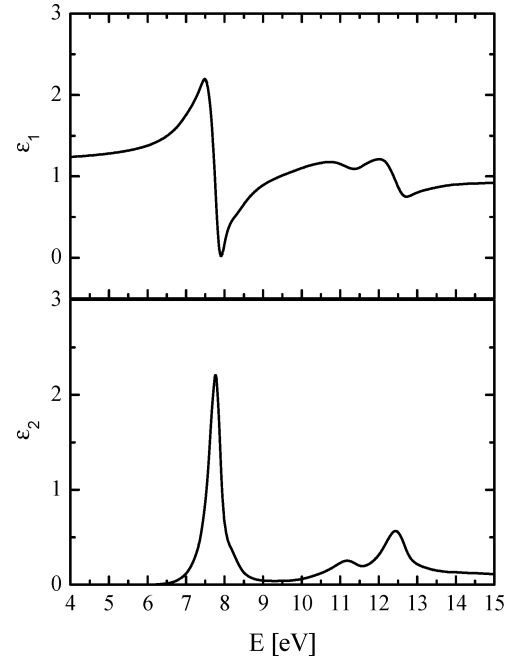

Figure 4. Calculated electronic dielectric spectra of liquid acetonitrile at ambient conditions. The real (top) and imaginary (bottom) parts of the complex function $\varepsilon = \varepsilon_1 - i\varepsilon_2$ are obtained as an average over 40 MC uncorrelated configurations, each one containing 100 CH_3CN molecules.

identifying these processes, since it is expected that they will depend strongly on the dynamical many-body effects.

Still within the linear-response theory of the optical absorption, the complex dielectric function $\varepsilon = \varepsilon_1 - i\varepsilon_2$ has a central role in excited states and provides a means of deducing the screened Coulomb interaction that is essential in the *GW* approximation.[31,33] Further, the $\varepsilon(\omega)$ spectra supply information about time and space scales of molecular events in fluids at thermal equilibrium. To evaluate the frequency dependency of the dielectric properties of liquid CH_3CN, we perform an average calculation over all 40 uncorrelated configurations. With this procedure, we include the polarization effects due to reorientation of the molecules, which is very important to describe the dielectric function of dipolar liquids.

The real part of the dielectric function ε_1 is obtained from the imaginary part ε_2 through the Kramers−Kronig relations. The behavior of both ε_1 and ε_2 as a function of the photon energy is outlined in Figure 4. The relative permittivity (ε_1) presents a damping around the valence transition energy, which can be attributable to the finite lifetime of the excited states. More importantly, the dielectric loss factor (ε_2) confirms that absorptions at this region are far from the static HOMO−LUMO gap, presenting a maximum at 7.8 eV.

Concluding Remarks

In the present study, we give an electronic-structure-based description of the dynamical dielectric response of liquid acetonitrile from ab initio calculations. Our findings reveal that the impact of intermolecular interactions leads to a decrease of the transition energies relative to the gas phase, which is consistent with condensed phase systems. Consequently, such effects produce differences in electron populations of the innermost states and differences in the mixing between valence and core states in the liquid phase. More generally, the calculations suggest that the features of the optical absorption spectrum of liquid CH_3CN depend on both their intermolecular interactions and ground-state electronic properties. Concerning the current method, we provide an efficient means to explore the dielectric properties of condensed phase systems consisting of large molecules.

Acknowledgment. This work has been supported by the Brazilian agencies CNPq (Grant No. 550311/2007-6) and FAPESB.

References and Notes

(1) Reimers, J. R.; Hall, L. E. *J. Am. Chem. Soc.* **1999**, *121*, 3730.
(2) Spangberg, D.; Hermansson, K. *Chem. Phys.* **2004**, *300*, 165.
(3) Shkrob, I. A.; Sauer, M. C., Jr. *J. Phys. Chem. A* **2002**, *106*, 9120.
(4) Xia, C.; Peon, J.; Kohler, B. *J. Chem. Phys.* **2002**, *117*, 8855.
(5) Mitsui, M.; Ando, N.; Kokubo, S.; Nakajima, A.; Kaya, K. *Phys. Rev. Lett.* **2003**, *91*, 153002.
(6) Leach, S.; Schwell, M.; Un, S.; Jochims, H. W.; Baumgaertel, H. *Chem. Phys.* **2008**, *344*, 147, and references therein.
(7) Reis, H.; Papadopoulos, M. G.; Avramopoulos, A. *J. Phys. Chem. A* **2003**, *107*, 3907.
(8) Avramopoulos, A.; Papadopoulos, M. G.; Reis, H. *J. Phys. Chem. B* **2007**, *111*, 2546.
(9) Wallacher, D.; Soprunyuk, V. P.; Knorr, K.; Kityk, A. V. *Phys. Rev. B* **2004**, *69*, 134207.
(10) Tomasi, J.; Mennucci, B.; Cammi, R. *Chem. Rev.* **2005**, *105*, 2999.
(11) Luo, Y.; Norman, P.; Agren, H.; Sylvester-Hvid, K. O.; Mikkelsen, K. V. *Phys. Rev. E* **1998**, *57*, 4778.
(12) Nigam, S.; Majumdera, C. *J. Chem. Phys.* **2008**, *128*, 214307.
(13) (a) Shelton, D. P.; Kaatz, P. *Phys. Rev. Lett.* **2000**, *84*, 1224. (b) Shelton, D. P. *J. Chem. Phys.* **2005**, *123*, 084502.
(14) Rivelino, R.; Cabral, B. J. C.; Coutinho, K.; Canuto, S. *Chem. Phys, Lett.* **2005**, *407*, 13.
(15) (a) Böhm, H.; McDonald, I. R.; Madden, P. A. *Mol. Phys.* **1983**, *49*, 347. (b) Grabuleda, X.; Jaime, C.; Kollman, P. A. *J. Comput. Chem.* **2000**, *21*, 901.
(16) (a) Jorgensen, W. L.; Briggs, J. M. *Mol. Phys.* **1988**, *63*, 547. (b) Hirata, Y. *J. Phys. Chem. A* **2002**, *106*, 2187.
(17) Prendergast, D.; Grossman, J. C.; Galli, G. *J. Chem. Phys.* **2005**, *123*, 014501.
(18) VandeVondele, J.; Mohamed, F.; Krack, M.; Hutter, J.; Sprik, M.; Parrinello, M. *J. Chem. Phys.* **2005**, *122*, 014515.
(19) Fernández-Serra, M. V.; Artacho, E. *Phys. Rev. Lett.* **2006**, *96*, 016404.
(20) Lee, H.-S.; Tuckerman, M. E. *J. Chem. Phys.* **2006**, *125*, 154507.
(21) Garbuio, V.; Cascella, M.; Reining, L.; Del Sole, R.; Pulci, O. *Phys. Rev. Lett.* **2006**, *97*, 137402.
(22) Rivelino, R.; de Brito Mota, F. *Nano Lett.* **2007**, *7*, 1526.
(23) (a) Coutinho, K.; Canuto, S. *J. Chem. Phys.* **2000**, *113*, 9132. (b) Canuto, S.; Coutinho, K.; Trzesniak, D. *Adv. Quantum Chem.* **2002**, *41*, 161. (c) Rivelino, R.; Canuto, S.; Coutinho, K. *Braz. J. Phys.* **2004**, *34*, 84.
(24) Economou, E. N. *Green's Functions in Quantum Physics*; Spring-Verlag: Berlin, 1983.
(25) Perdew, J. P.; Burke, K.; Ernzerhof, M. *Phys. Rev. Lett.* **1996**, *77*, 3865.
(26) (a) Troullier, N.; Martins, J. L. *Phys. Rev. B* **1991**, *43*, 1993. (b) Kleinman, L.; Bylander, D. M. *Phys. Rev. Lett.* **1982**, *48*, 1425.
(27) (a) Ordejon, P.; Artacho, E.; Soler, J. M. *Phys. Rev. B* **1996**, *53*, R10441. (b) Soler, J. M.; Artacho, E.; Gale, J. D.; Garcia, A.; Junquera, J.; Ordejon, P.; Sanchez-Portal, D. *J. Phys.: Condens. Matter* **2002**, *14*, 2745, and references therein.
(28) Coutinho K.; Canuto, S. *DICE, A Monte Carlo Program for Molecular Liquid Simulation*; University of São Paulo: São Paulo, Brazil, 2003.
(29) The MC simulation is carried out in a cubic box with side $L = 34$ Å, and the usual periodic boundary conditions with minimum image convention are applied. The size of the simulation cell is varied to reproduce the density of the liquid. After the thermalization stage of 2×10^7 MC steps, the averaging stage of 5×10^7 MC steps is performed. The calculated average density is 798 g cm^{-3}, comparable with the available experimental density of 0.777 g cm^{-3} (see ref 16b).
(30) The band gap is calculated as an average difference between the KS eigenvalues of the highest occupied molecular orbital (HOMO) and lowest unoccupied molecular orbital (LUMO) of the ground-state electronic structure of the fluid phase, including all uncorrelated structures.
(31) Hahn, P. H.; Schmidt, W. G.; Seino, K.; Preuss, M.; Bechstedt, F.; Bernholc, J. *Phys. Rev. Lett.* **2005**, *94*, 037404.
(32) Onida, G.; Reining, L.; Rubio, A. *Rev. Mod. Phys.* **2002**, *74*, 601.
(33) Lu, D.; Gygi, F.; Galli, G. *Phys. Rev. Lett.* **2008**, *100*, 147601.

JP902549Y